A&A manuscript no.
(will be inserted by hand later)

Your thesaurus codes are:
09(09:07:1;09:03:1;08:06:2;02:05:1)

ASTRONOMY
AND
ASTROPHYSICS

arXiv:astro-ph/0001274v1 15 Jan 2000

Neutrino decay and the thermochemical equilibrium of the interstellar medium

Néstor M. Sánchez D.[1,2] **and Neyda Y. Añez P.**[1]

[1] Departamento de Física, Facultad Experimental de Ciencias, Universidad del Zulia, Maracaibo, Venezuela
[2] Centro de Astrofísica Teórica, Facultad de Ciencias, Universidad de los Andes, Mérida, Venezuela

Received 23 September 1999 / Accepted 23 December 1999

Abstract. We calculate the thermochemical equilibrium of the diffuse interstellar medium, including ionization by a photon flux F_ν from neutrino decay. The main heating mechanism considered is photoelectrons from grains and PAHs. For the studied range of F_ν values, there always exists two regions of stability (a warm and a cold phase) that can coexist in equilibrium if the thermal interstellar pressure is between a maximum value (P_{max}) and a minimum value (P_{min}). High F_ν values ($\sim 10^4 - 10^5$ cm^{-2} s^{-1}) can be consistent with observed interstellar pressures only if more efficient sources are heating the gas. It is shown that a neutrino flux increase (due, for example, to an increase in the supernova explosion rate) may stimulate the condensation of cold gas by decreasing P_{max} below the interstellar pressure value.

Key words: ISM: general – ISM: clouds – stars: formation – elementary particles

1. Introduction

The diffuse interstellar medium (ISM) is observed to be inhomogeneous with cold ($T \lesssim 10^2$ K) clouds embedded in a warmer ($T \sim 10^4$ K) intercloud gas (see, for example, the review of Kulkarni & Heiles 1988). The theoretical explanation for this structure was provided by Field et al. (1969) who showed that two thermally stable phases can coexist in pressure equilibrium over a limited range of pressures, close to those observed in the ISM. Since the two-phase model of Field et al. (1969), the thermal and ionization equilibrium of the ISM and its stability have been studied by many authors including different heating and ionizing processes (Black 1987; Kulkarni & Heiles 1988). The response of the ISM to variations in physical processes and parameters are of interest both to a better understanding of the ISM behavior and because of its central role in star formation and galaxy evolution models. Effects on the ISM equilibrium of variations in, for example, X-ray and far UV radiation fields, cosmic ray ionization and metal abundance have been studied by several authors (Shull & Woods 1985; Parravano 1987; Wolfire et al. 1995; Parravano & Pech 1997). In this work, we are interested in a particular process: the flux of ionizing photons coming from the radiative decay of neutrinos (Sciama 1990). Notwithstanding this is a speculative theory, Sciama has argued in a set of papers (Sciama 1993, 1995, 1997a, 1997b, 1998) that it can explain the widespread ionization far from the galactic disk and many other observational results. The simplification in Sciama's work is to assume a temperature of $\sim 10^4$ K without explicitly solving the thermal equilibrium. The former was made by Dettmar & Schulz (1992) who showed that heat input associated with neutrino decay is too small to account for the observed ISM temperature. However, their conclusion that neutrino decay cannot be a dominant source of ionization could be mistaken, as was pointed out by Sciama (1993), because they neglected the existence of other known heating mechanisms. Our goal here is to analize, in a more complete and self-consistent way, the effect of ionization due to neutrino decay on the thermochemical equilibrium of the ISM.

In Sect. 2 we discuss the physical processes included in this work and provide the basic equations. Sect. 3 is dedicated to a discussion of the results, and the main conclusions are summarized in Sect. 4.

2. Basic equations

In order to analize the effect of neutrino decay photons on the thermochemical equilibrium, a simple model for the ISM is used. The included cooling mechanisms are: a) cooling by collisions of electrons with C$^+$, Si$^+$, Fe$^+$, O$^+$, S$^+$ and N (Λ_e); b) cooling by collisions of neutral hydrogen with Si$^+$, Fe$^+$ and C$^+$ (Λ_H); and c) cooling due to Ly-α excitation by electrons (Λ_{Ly}). All the cooling rates and the relative abundances were taken from Dalgarno & McCray (1972). We consider the following heating mechanisms:
a) Interaction of cosmic ray with hydrogen atoms and elec-

Send offprint requests to: N. Sánchez
Correspondence to: nestor@orion.ciens.luz.ve

trons:

$$\Gamma_{cr} = \zeta_{cr}\left[5\times10^{-12}(1+\Phi)n(1-\chi) + 5.1\times10^{-10}n_e\right] \text{ ergs cm}^{-3}\text{ s}^{-1}\ , \quad (1)$$

where $n = n(\mathrm{HI}) + n(\mathrm{HII})$ is the total number density of hydrogen, n_e is the number density of electrons and $\chi = n(\mathrm{HII})/n$ is the ionization degree of hydrogen. The number of secondary ionizations (Φ) was taken from Dalgarno & McCray (1972), and the primary ionization rate is assumed to be $\zeta_{cr} = 10^{-17}$ s^{-1} (Spitzer 1978; Black et al. 1990; Webber 1998).

b) Heating by H_2 formation on dust grains (Spitzer 1978):

$$\Gamma_H = 4.4\times10^{-29}n^2(1-\chi) \text{ ergs cm}^{-3}\text{ s}^{-1}\ . \quad (2)$$

c) Photoelectric heating from small grains and PAHs (Bakes & Tielens 1994):

$$\Gamma_{pe} = 10^{-24}\epsilon G_o n \text{ ergs cm}^{-3}\text{ s}^{-1}\ , \quad (3)$$

where the heating efficiency (ϵ) is given by

$$\epsilon = \frac{4.87\times10^{-2}}{\left[1+4\times10^{-3}\left(G_oT^{1/2}/n_e\right)^{0.73}\right]} + \frac{3.65\times10^{-2}\left(T/10^4\right)^{0.7}}{\left[1+2\times10^{-4}\left(G_oT^{1/2}/n_e\right)\right]}\ , \quad (4)$$

and G_o is the far UV field normalized to its solar neighborhood value.

We only consider ionization/recombination for hydrogen. The recombination rate is given by

$$X^+ = \chi n_e \alpha(T) \text{ s}^{-1}\ , \quad (5)$$

where $\alpha(T)$ is the recombination coefficient to all states except the ground one, and it was taken from Spitzer (1978). The rate of ionization by cosmic rays is given by

$$X^-_{cr} = \zeta_{cr}(1+\phi)(1-\chi) \text{ s}^{-1}\ . \quad (6)$$

We also use the simple analytic fits provided by Wolfire et al. (1995) to estimate the ionization (X^-_{XR}) and heating (Γ_{XR}) due to the soft X-ray background as functions of the column density (N_w) and the electron fraction (n_e/n). In this work we adopt $N_w = 10^{19}$cm^{-2}.

In addition to the above sources of ionization, we also consider the photons produced by neutrino decay. The ionization due to this mechanism can be written in the form (Sciama 1990):

$$X^-_\nu = F_\nu\sigma(1-\chi) \text{ s}^{-1}\ , \quad (7)$$

where $\sigma = 6.3\times10^{-18}$ cm^2 is the absorption cross section of hydrogen and F_ν is the flux of hydrogen-ionizing photons produced by neutrino decay. In this work F_ν is a free parameter, although Sciama (1997a) estimated that a value of $F_\nu \simeq 3\times10^4$ photons cm^{-2} s^{-1} is necessary to produce an electron density $n_e \sim 0.05$ cm^{-3} in the intercloud medium. The most recent (but still uncertain) estimation was $F_\nu \lesssim 10^5$ photons cm^{-2} s^{-1} (Sciama 1998).

3. Results and discussion

The thermochemical equilibrium is calculated by solving simultaneously the equations $\Lambda = \Gamma$ and $X^+ = X^-$, where $\Lambda = \Lambda_e + \Lambda_H + \Lambda_{Ly}$ is the total cooling rate, $\Gamma = \Gamma_{cr} + \Gamma_H + \Gamma_{pe} + \Gamma_{XR}$ is the total heating rate, and $X^- = X^-_{cr} + X^-_{XR} + X^-_\nu$ is the total ionization rate. Fig. 1a shows the equilibrium pressure-density relations for $G_o = 1$ and for three different values of F_ν (0, 10^2 and 10^4 cm^{-2} s^{-1}). The corresponding electron fractions (n_e/n) are showed in Fig. 1b, where it can be seen that, as expected, n_e/n increases as F_ν increases. Most of the ionization for the cases $F_\nu > 10$ cm^{-2} s^{-1} is due to photons coming from neutrino decay, and thus the neutrino decay is a very efficient ionization mechanism. An increase in F_ν (and the consequent increase in the electron density) enhances the cooling by electron collisions (Λ_e). Additionally, the dominant heating mechanism is always photoelectrons from grains and PAHs (Γ_{pe}), which almost it is not affected by the flux F_ν. Consequently, for a given density, when F_ν increases the thermal equilibrium is reached at lower temperatures in the regions where Λ_e dominates the cooling (high densities), and the equilibrium curve is shifted down (see Fig. 1a). In contrast, at low densities ($n \sim 10^{-2}$ cm^{-3}), the dominant cooling mechanism is Λ_{Ly}, which decreases when F_ν increases and, in this case, the equilibrium is reached at higher temperatures.

Fig. 1a also shows that two regions of thermal stability, i.e., where the slope is positive (Field 1965), always exist and two phases can coexist in pressure equilibrium if the interstellar pressure $P \equiv p/k$ is between a minimum (P_{min}) and a maximum (P_{max}) value. For the case $F_\nu = 0$ we obtain $P_{max} \simeq 1100$ K cm^{-3} and $P_{min} \simeq 490$ K cm^{-3}; and if we assume an equilibrium pressure of $P \simeq 10^3$ K cm^{-3}, then there can be gas with $T \simeq 8800$ K, $n \simeq 0.1$ cm^{-3} and $n_e/n \simeq 4.7\times10^{-2}$, and gas with $T \simeq 100$ K, $n \simeq 10$ cm^{-3} and $n_e/n \simeq 1.7\times10^{-3}$ coexisting in equilibrium. These results agree roughly with observational estimations of the warm and cold neutral phases in the local ISM (Kulkarni & Heiles 1988). Furthermore, it can be seen in Fig. 1a that P_{max}, the maximum pressure value over which only the cold phase can exist, decreases as F_ν increases. For $F_\nu = 10^2$ cm^{-2} s^{-1} and for $F_\nu = 10^4$ cm^{-2} s^{-1} we obtain $P_{max} \sim 640$ K cm^{-3} and $P_{max} \sim 500$ K cm^{-3}, respectively; but observations indicate that the pressure in most of the regions of the Galactic plane is $\gtrsim 10^3$ K cm^{-3} (Jenkins et al. 1983). Therefore, there seems to be an inconsistency between the observed pressure in a multi-phase medium and high F_ν values. The basic reason for this behavior (that high F_ν values imply too low P_{max} values) is that neutrino decay is a poor heating agent, while other processes can ionize *and* heat the ISM. For instance, when the cosmic ray ionization rate (ζ_{cr}) is changed (keeping $F_\nu = 0$ fixed), we find that P_{max} decreases as ζ_{cr} increases, but for $\zeta_{cr} \gtrsim 10^{-16}$ s^{-1} the heating by cosmic rays (Γ_{cr}) becomes more important that heating by photoelectrons from grains and PAHs (Γ_{pe}), and then P_{max} begins to increase as ζ_{cr} is increased. The minimum P_{max} value is ~ 900 K cm^{-3}.

However, more efficient heating mechanisms that those considered here can rise up the equilibrium curve increasing P_{max}. In order to illustrate this effect, we have plotted in Fig. 2 P_{max} as a function of F_ν for three different values of G_o (1, 10 and 20) and, in consequence, three different values of Γ_{pe} (believed to be an important heating mechanism in the ISM). We can see that as F_ν is increased P_{max} decreases until a minimum value (~ 480 K cm^{-3} for $G_o = 1$, ~ 590 K cm^{-3} for $G_o = 10$ and ~ 660 K cm^{-3} for $G_o = 20$) and after that remains constant. This occurs when $n_e/n \rightarrow 1$ in the warm gas and, therefore, additional increases in F_ν do not produce additional changes in this phase. Fig. 2 shows that if an ISM pressure of $\sim 10^3$ K cm^{-3} is assumed, a two-phase medium is possible for $G_o = 1$ only if $F_\nu \lesssim 10$ cm^{-2} s^{-1}, and for $G_o = 20$ only if $F_\nu \lesssim 200$ cm^{-2} s^{-1}. We conclude that high fluxes of neutrino decay photons ($\gtrsim 10^3$ cm^{-2} s^{-1}) can be consistent with a two-phase medium only if more efficient heating sources are acting on the gas.

Sciama (1997a) estimated that $F_\nu \sim 3 \times 10^4$ cm^{-2} s^{-1} is necessary to produce $n_e \sim 0.05$ cm^{-3} at $T \sim 6000$ K. Fig. 3 shows n_e as function of F_ν for $T = 6000$ K and for the same three values of G_o given in Fig. 2. The desired electron density at this temperature can be reached at high F_ν values only if $G_o \gtrsim 20$ and, again, more efficient heating sources seem to be necessary.

An interesting consequence has to be noted: *neutrino beams from neighboring regions may induce the condensation of cold clouds stimulating the formation of stars.* The importance of star formation triggered by previously formed stars has been recognized by many authors (see the review of Elmegreen 1992). Triggering mechanisms are usually related to compression of the ISM by shock waves from close supernovas, because the transition warm gas → cold gas is promoted if the ISM pressure rises over P_{max}. Although this kind of mechanism can act only over short distances (compared with the Galaxy size) it can propagate over large scales, and the idea of self-propagated star formation has been used to study the formation of spatial patterns in galactic disks (Mueller & Arnett 1976; Gerola & Seiden 1978; Seiden & Gerola 1979; Schulman & Seiden 1990; Jungwiert & Palous 1994). However, the phase transition warm gas → cold clouds can be also obtained by decreasing P_{max} under P (assumed constant) if the local flux of decaying neutrinos increases due, for example, to an increase in the supernova explosion rate. This triggering mechanism depends on the propagation of neutrinos, and therefore can act over large distances in short time intervals. On the other hand, star formation can also inhibit in different ways the warm gas condensation self-regulating the star formation process inclusively over large distances (Cox 1983; Franco & Shore 1984; Struck-Marcell & Scalo 1987; Parravano 1988, 1989). It has been shown that star formation inhibition (rather than stimulation) can also contribute to the formation and maintenance of spatial patterns in galaxies (Freedman & Madore 1984; Chappell & Scalo 1997). Stimulation and inhibition mechanisms of star formation must be acting simultaneously in the Galaxy, but it is not clear yet what spatial scales are important for each one. The effect of *non-local* star formation stimulation on the formation of spiral patterns in galaxies should be analysed in future models.

4. Conclusions

The thermochemical equilibrium of the ISM, including decay of neutrinos into an ionizing photon flux F_ν, was calculated. The range $0 \leq F_\nu \leq 10^5$ cm^{-2} s^{-1} always shows two regions of stability (a warm and a cold phase) that can coexist in equilibrium if the ISM pressure is below a threshold value (P_{max}). High F_ν values ($\sim 3 \times 10^4$ cm^{-2} s^{-1}) estimated by Sciama (1997a) to produce $n_e \simeq 0.05$ cm^{-3} at $T \simeq 6000$ K, only can be consistent with observed ISM pressures if more efficient processes are heating the gas. It also was showed that a neutrino flux increase (due, for example, to an increase in the supernova explosion rate) may stimulate the condensation of cold gas (and probably the star formation) by decreasing P_{max} under the ISM pressure value.

Acknowledgements. This work has been partially supported by CONDES of Universidad del Zulia. The authors are very grateful to an anonymous referee for several helpful suggestions, and to Cesar Mendoza for his assistance in the manuscript preparation.

References

Bakes E.L.O., Tielens A.G.G.M., 1994, ApJ 427, 822.
Black J.H., 1987, in Interstellar Processes, eds. Hollenbach D.J., Thronson H.A. (Dordrecht: Reidel), 731.
Black J.H., van Dishoeck E.F., Willner S.P., Woods R.C., 1990, ApJ 358, 459.
Chappell D.W., Scalo J., 1997, astro-ph/9706161.
Cox D.P., 1983, ApJ 265, L61.
Dalgarno A., McCray R.A., 1972, ARA&A 10, 375.
de Jong T., 1977, A&A 55, 137.
Dettmar R.-J., Schulz H., 1992, A&A 254, L25.
Draine B.T., 1978, ApJS, 36, 595.
Elmegreen B.G., 1992, in Star Formation in Stellar Systems, eds. Tenorio-Tagle G., Prieto M., Sánchez F. (Cambridge: Cambridge University Press), 515.
Field G.B., 1965, ApJ 142, 531.
Field G.B., Goldsmith D.W., Habing H.J., 1969, ApJ 155, L149.
Franco J., Shore S.N., 1984, ApJ 285, 813.
Freedman W.L., Madore B.F., 1984, ApJ 280, 592.
Gerola H., Seiden P.E., 1978, ApJ 223, 129.
Jenkins E.B., Jura M., Loewenstein M., 1983, ApJ 270, 88.
Jungwiert B., Palous J., 1994, A&A 187, 55.
Jura M., 1976, ApJ 204, 12.

Kulkarni S.R., Heiles C., 1988, in Galactic and Extragalactic Radio Astronomy, eds. Verschuur G.L., Kellermann K.I. (New York: Springer), 95.
Mueller M.W., Arnett W.D., 1976, ApJ 210, 670.
Parravano A., 1987, A&A 172, 280.
Parravano A., 1988, A&A 205, 71.
Parravano A., 1989, ApJ 347, 812.
Parravano A., Pech C., 1997, A&A 327, 1262.
Schulman L.S., Seiden P.E., 1990, Advances in Physics 39, 1.
Sciama D.W., 1990, ApJ 364, 549.
Sciama D.W., 1993, ApJ 409, L25.
Sciama D.W., 1995, ApJ 448, 667.
Sciama D.W., 1997a, ApJ 488, 234.
Sciama D.W., 1997b, MNRAS 289, 945.
Sciama D.W., 1998, A&A 335, 12.
Seiden P.E., Gerola H., 1979, ApJ 233, 56.
Shull J.M., Woods D.T., 1985, ApJ 288, 50.
Spitzer L., 1978, Physical Processes in the Interstellar Medium (New York: Wiley).
Struck-Marcell C., Scalo J.M., 1987, ApJS 64, 39.
van Dishoeck E., Black J.H., 1991, ApJ 369, L9.
Webber W.R., 1998, ApJ 506, 329.
Wolfire M.G., Hollenbach D., McKee C.F., Tielens A.G.G.M., Bakes E.L.O., 1995, ApJ 443, 152.

Figure captions

Fig. 1a. Thermal pressure as a function of the total hydrogen density in equilibrium for $G_o = 1$ and for $F_\nu = 0$ (solid line), $F_\nu = 10^2$ (dashed line) and $F_\nu = 10^4$ cm^{-2} s^{-1} (dot-dashed line).

Fig. 1b. The electron fraction as a function of the total hydrogen density in equilibrium for $G_o = 1$ and for $F_\nu = 0$ (solid line), $F_\nu = 10^2$ (dashed line) and $F_\nu = 10^4$ cm^{-2} s^{-1} (dot-dashed line).

Fig. 2. The maximum pressure P_{max} for the coexistence of warm and cold gas as a function of F_ν for $G_o = 1$ (solid line), $G_o = 10$ (dashed line) and $G_o = 20$ (dot-dashed line).

Fig. 3. The electron density as a function F_ν for $T = 6000$ K and for $G_o = 1$ (solid line), $G_o = 10$ (dashed line) and $G_o = 20$ (dot-dashed line).

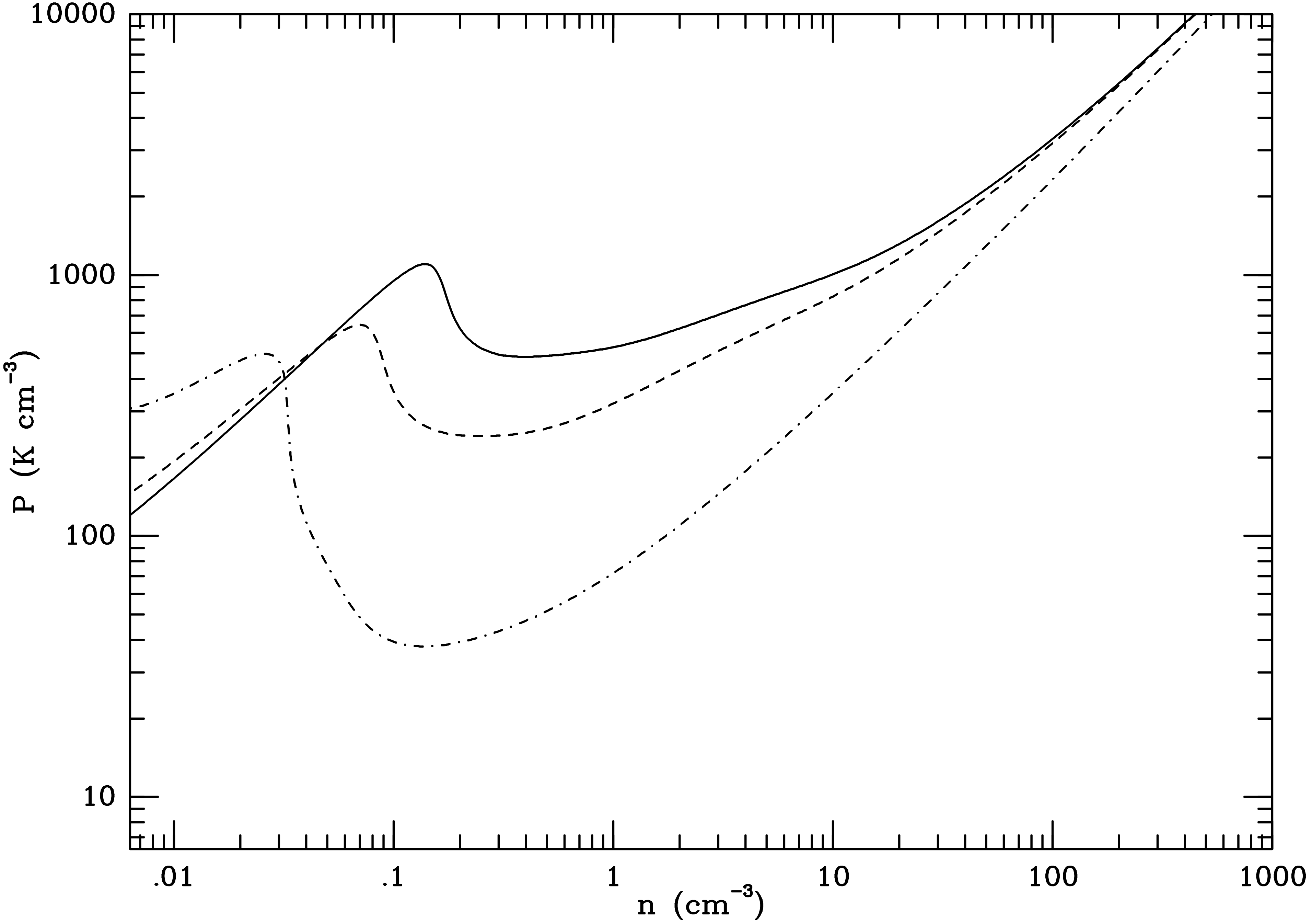
10000
1000
100
10
P (K cm^{-3})
.01
.1
1
10
100
1000
n (cm^{-3})

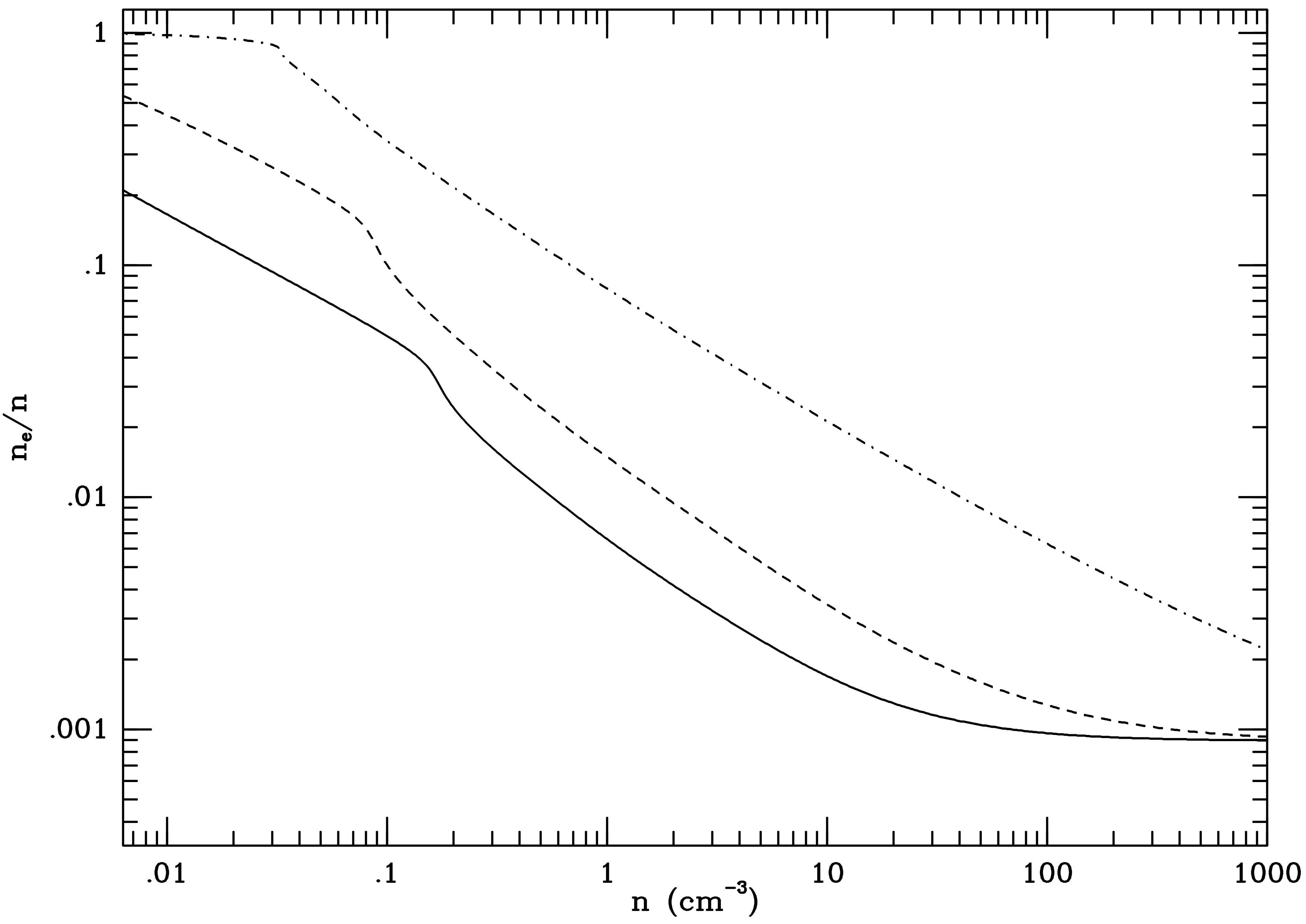
1
.1
.01
.001
n_e/n
.01
.1
1
10
100
1000
n (cm^{-3})

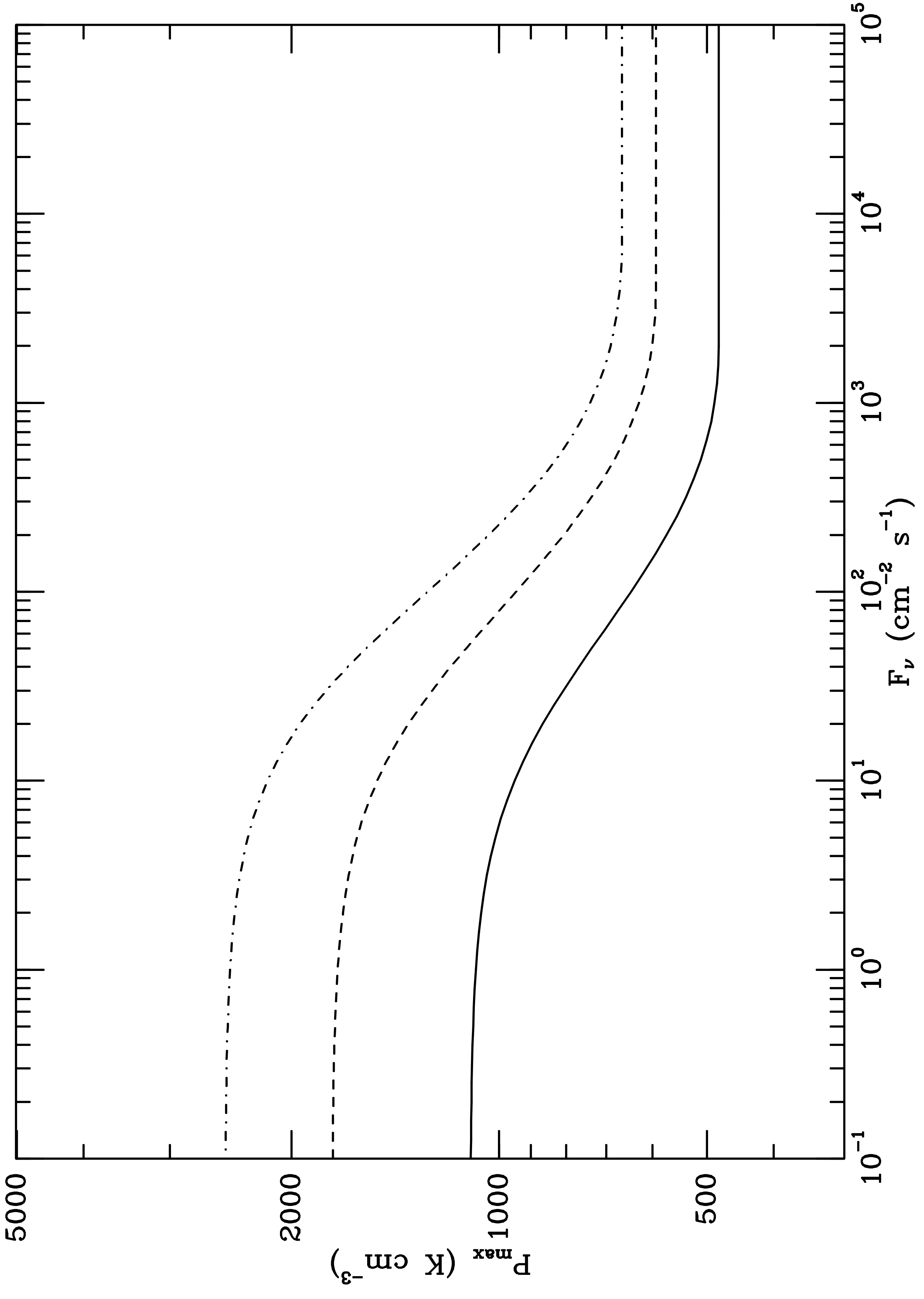
P_{max} (K cm^{-3})
500
1000
2000
5000
F_ν (cm^{-2} s^{-1})
10^{-1}
10^{0}
10^{1}
10^{2}
10^{3}
10^{4}
10^{5}

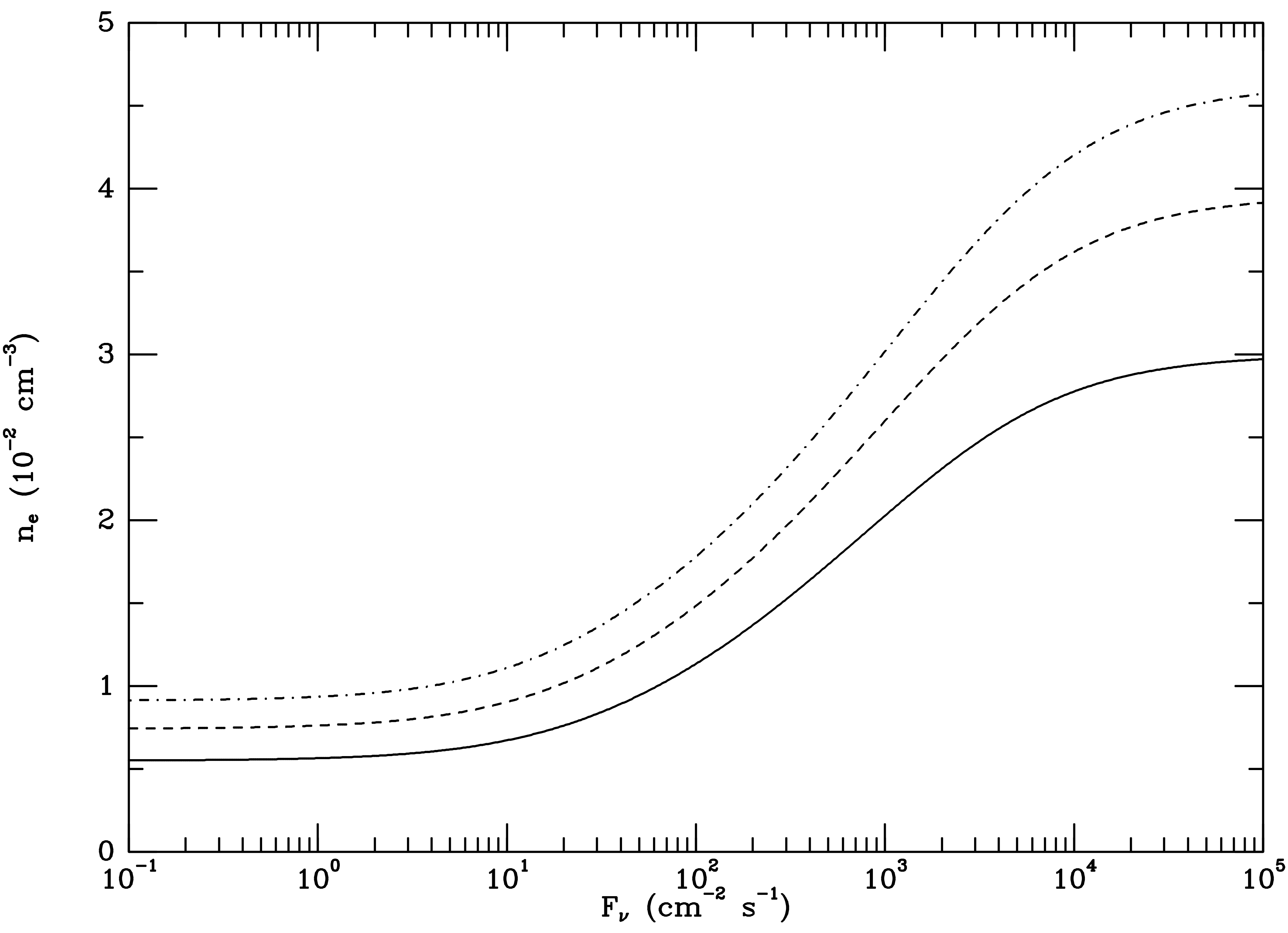

n_e $(10^{-2}$ cm$^{-3})$
0
1
2
3
4
5
10^{-1}
10^{0}
10^{1}
10^{2}
10^{3}
10^{4}
10^{5}
F_ν (cm^{-2} s^{-1})